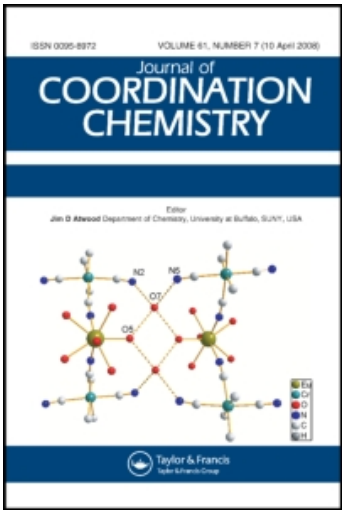

Journal of Coordination Chemistry
Publication details, including instructions for authors and subscription information:
http://www.informaworld.com/smpp/title~content=t713455674

Binuclear copper(II) and oxovanadium(IV) complexes with 2,6-diformyl-4-tert-butylphenol-bis-(1'-phthalazinylhydrazone). Synthesis, properties and quantum chemical study

L. D. Popov[a]; I. N. Shcherbakov[a]; S. I. Levchenkov[b]; Y. P. Tupolova[a]; V. A. Kogan[a]; V. V. Lukov[a]
[a] Department of Chemistry, Rostov State University, Russian Federation [b] Department of Physical Organic Chemistry, Southern Scientific Centre of the RAS, 41, Rostov-on-Don, Russia

First published on: 19 September 2007

To cite this Article Popov, L. D. , Shcherbakov, I. N. , Levchenkov, S. I. , Tupolova, Y. P. , Kogan, V. A. and Lukov, V. V.(2008) 'Binuclear copper(II) and oxovanadium(IV) complexes with 2,6-diformyl-4-**tert**-butylphenol-**bis**-(1'-phthalazinylhydrazone). Synthesis, properties and quantum chemical study', Journal of Coordination Chemistry, 61: 3, 392 — 409, First published on: 19 September 2007 (iFirst)
To link to this Article: DOI: 10.1080/00958970701338796
URL: http://dx.doi.org/10.1080/00958970701338796

Journal of Coordination Chemistry
Vol. 61, No. 3, 10 February 2008, 392–409

Taylor & Francis
Taylor & Francis Group

Binuclear copper(II) and oxovanadium(IV) complexes with 2,6-diformyl-4-*tert*-butylphenol-*bis*-(1′-phthalazinylhydrazone). Synthesis, properties and quantum chemical study

L. D. POPOV†, I. N. SHCHERBAKOV*†, S. I. LEVCHENKOV‡, Y. P. TUPOLOVA†, V. A. KOGAN† and V. V. LUKOV†

†Department of Chemistry, Rostov State University, 7, Zorge Str., Rostov-on-Don, 344019, Russian Federation
‡Department of Physical Organic Chemistry, Southern Scientific Centre of the RAS, 41, Chekhova Str., 344006, Rostov-on-Don, Russia

(*Received 29 November 2006; in final form 31 January 2007*)

Four binuclear transition metal complexes: $[Cu_2L(\mu\text{-}OCH_3)]\cdot CH_3OH$, $[Cu_2H_2L(\mu\text{-}Cl)Cl_2]\cdot(CH_3OH)$, $[Cu_2H_2L(\mu\text{-}Br)Br_2]\cdot(CH_3OH)$, $[(VO)_2H_2L(\mu\text{-}Cl)]Cl_2\cdot(CH_3OH)$ were synthesized by reaction of the Robson-type binucleating ligand H_3L (2,6-diformyl-4-*tert*-butylphenol-*bis*-(1′-phthalazinylhydrazone)) with Cu(II) acetate, $CuCl_2$, $CuBr_2$ and $VOCl_2$, correspondingly. IR and ESR spectra, elemental analysis, conductivity measurements, magnetochemical study and DFT calculations were used to characterize the ligand and isolated complexes. The ligand is a NNONN donor and its degree of deprotonation varies with the metal salt used for reaction (triply deprotonated form L^{-3} is observed in reaction with copper(II) acetate, while monodeprotonated form H_2L^- is found in complexes obtained from metal halides). All complexes contain an endogenous phenoxide bridge and an exogenous methoxide, chloride or bromide bridge. Magnetic data reveal existence of antiferromagnetic interactions between the metal ions (experimental $2J$ values are -700, -73, -50 and $-190\,cm^{-1}$, correspondingly). Broken symmetry approach at the UB3LYP/6-31G(d) level was used to theoretically calculate spin-spin coupling between metal centers. Obtained values -570, -62, -53 and $-214\,cm^{-1}$ are rather close to experimental ones and reproduce their counterrelation. Spin density distribution in the singlet and triplet states of the complexes is discussed.

Keywords: Binuclear transition metal complexes; Broken symmetry approach; Magnetic exchange; Magnetochemistry; Quantum chemical calculations

1. Introduction

Hydrazones of polyfunctional carbonyl compounds are of particular interest for transition metal coordination chemistry. Acting as ligands they easily form bi- and polynuclear coordination compounds that can serve as reliable models for study of magnetic exchange interactions between paramagnetic centers [1–7]. Exceptionally useful in this respect are *bis*-hydrazones of 2,6-diformyl-4-R-phenols, pioneered by Robson [8–10] (so called Robson-type ligands), due to their structure predetermining

*Corresponding author. Email: shcherbakov@rsu.ru

ISSN 0095-8972 print/ISSN 1029-0389 online © 2008 Taylor & Francis
DOI: 10.1080/00958970701338796

formation of binuclear complexes with a wide variety of metal ions. By altering synthetic conditions complexes with mono-, di- and triply deprotonated hydrazone moieties can be obtained [11–14]. Exogenic bridging group of the binuclear complexes can be varied too, because this position is occupied by the anion of the metal salt used for complexation with the *bis*-hydrazone, μ-hydroxy or μ-alkoxy moiety [4, 5, 15–17]. Numerous studies of transition metal complexes (primarily copper(II)) with such ligands led to formulation of some general rules which can be used to predict structure and magnetic behavior [18–20]. Additional substantial interest to *bis*-hydrazones of 2,6-diformyl-4-R-phenols is evoked by their potential biological activity [21, 22].

Analysis of the current literature shows that transition metal complexes with *bis*-hetarylhydrazones are not so systematically studied as complexes with *bis*-acylhydrazones, *bis*-semicarbazones, *bis*-thiosemicarbazones and their analogues, though presence of heteroaromatic fragment in the ligand system is known to influence significantly magnetic exchange in compounds [19, 20, 23]. In the current article we report synthesis, physical–chemical and quantum–chemical investigation of the structure and properties of copper(II) and oxovanadium(IV) complexes of 2,6-diformyl-4-*tert*-butylphenol-*bis*-(1′-phthalazinylhydrazone).

2. Experimental

2.1. *Materials and methods*

All chemicals used were of reagent grade. Solvents were dried and distilled before use according to standard procedures. 2,6-Diformyl-4-*tert*-butylphenol was prepared by a known method [24]. 1′-Phthalazinylhydrazine hydrochloride was purchased from Aldrich and used without further purification. Metal salts were used in their hydrated forms, i.e., $Cu(CH_3COO)_2 \cdot 2H_2O$, $CuCl_2 \cdot 2H_2O$, $CuBr_2 \cdot 2H_2O$; oxovanadium(IV) dichloride was used as a 40% aqueous solution.

2.2. *Synthesis of 2,6-diformyl-4-*tert*-butylphenol-bis-(1′-phthalazinylhydrazone) (H_3L, 1)*

To a hot suspension of 1′-phthalazinylhydrazine hydrochloride (0.04 mol) in ethanol (40 mL) was added hot solution of 2,6-diformyl-4-*tert*-butylphenol (0.08 mol) in ethanol (20 mL). After 5 min, sodium acetate (0.04 mol) was added and the mixture was heated under reflux for 4 h. The precipitated yellow crystalline solid was filtered off, washed with water and hot methanol, and dried *in vacuo*. Product was recrystallized from DMF–ethanol mixture (Yield: 65%, m.p. >250°C).

^{1}H-NMR (DMSO-d^6): 1.40 (s, 9H, -*tert*-Bu), 7.60–7.74 (multiplet, 6H, aromatic H^5–H^7 of phthalazine moieties), 7.86 (s, 2H, aromatic H adjacent to -*tert*-Bu), 7.98 (broad singlet, 2H, aromatic H^4 of phthalazine moiety), 8.36 (d, broad, $J = 6.81$ Hz, 2H, aromatic H^8 of phthalazine moiety), 8.72 (s, 2H, H–C=N), 11.0 (s, 1H, OH, D_2O exchangeable), 12.1 (s, 2H, NH, D_2O exchangeable).

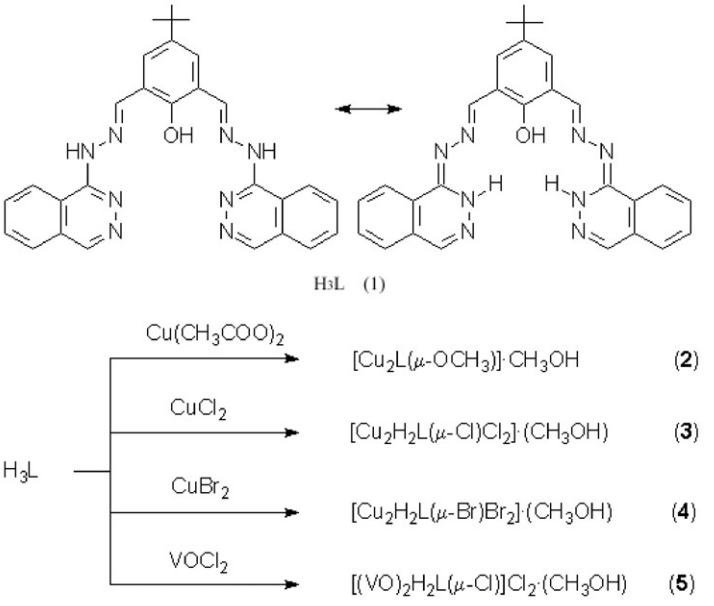

Scheme 1.

2.3. *Synthesis of complexes 2–5*

By reaction of 2,6-diformyl-4-*tert*-butylphenol-*bis*-(1′-phthalazinylhydrazone) (**1**, H_3L) with copper(II) acetate, copper(II) chloride, copper(II) bromide and oxovanadium(IV) dichloride, metal complexes **2**–**5** were isolated (see scheme 1).

All metal complexes under study were synthesized by standard procedure (as follows).

To a hot suspension of 2,6-diformyl-4-*tert*-butylphenol-*bis*-(1′-phthalazinylhydrazone) (0.002 mol) in methanol (20 mL) was added hot solution of metal salt (0.004 mol) in methanol (10 mL); upon addition *bis*-hydrazone immediately dissolved. A mixture was heated under reflux for 2 h. The precipitate, which separated after cooling, was filtered off, washed with methanol, and dried *in vacuo*. All complexes were recrystallized from methanol. Yield, analytical and physical data of the complexes are shown in table 1.

2.4. *Analysis and physical measurements*

The complexes were analyzed by EDTA titration after decomposition with a mixture of HCl and $HClO_4$. Microanalysis on C, H and N was performed on a Perkin-Elmer 240C analyzer. The ^{1}H-NMR spectra were recorded in the 0–15 ppm range in DMSO-d^6 solvent on a Varian 300 MHz spectrometer at room temperature using TMS as internal reference. Infrared spectra were obtained on a UNICAM SP1200 spectrometer in a KBr matrix in the range 4000–400 cm^{-1}. Room and liquid nitrogen temperature ESR spectra were obtained with an ER-9 (Zeiss) spectrometer. Magnetic susceptibility of powdered samples of the complexes was measured in the temperature range 300–77.4 K using

Table 1. Analytical, physical and molar conductance data for **1**–**5**.

Compound	Empirical formula	Found (Calcd) %				M.p. (°C)	λ_m ($\Omega^{-1}cm^2mol^{-1}$)	Color (yield %)
		C	H	N	M			
1	$C_{28}H_{26}N_8O$	68.2 (68.6)	5.47 (5.34)	22.9 (22.8)	–	>250	–	Yellow (65)
2	$C_{30}H_{30}Cu_2N_8O_3$	53.0 (53.2)	4.50 (4.46)	16.3 (16.5)	18.5 (18.8)	>250	3	Brown (50)
3	$C_{29}H_{29}Cl_3Cu_2N_8O_2$	46.3 (46.1)	3.80 (3.87)	14.5 (14.8)	16.6 (16.8)	>250	19	Green (40)
4	$C_{29}H_{29}Br_3Cu_2N_8O_2$	39.9 (39.2)	3.36 (3.29)	12.5 (12.6)	14.5 (14.3)	>250	11	Green (45)
5	$C_{29}H_{29}Cl_3N_8O_4V_2$	45.4 (45.7)	3.92 (3.83)	14.9 (14.7)	13.6 (13.4)	>250	120	Brown (40)

a Faraday magnetometer employing magnetic field strength 0.9 T. Corrections were made for diamagnetic contributions of the samples according to Pascal's constants [25] and for temperature independent paramagnetism. The instrument was calibrated with the use of $Hg[Co(CNS)_4]$. Conductance was determined for DMF solutions (10^{-3} M) of the complexes using a R38 conductivity bridge.

2.5. *Computational details*

Quantum chemistry modelling of the ligand and complexes electronic structure was performed employing the DFT approach. Model ligand designed for calculations was derived from *bis*-hydrazone (**1**) by substituting *tert*-butyl group with hydrogen in order to minimize computational costs. Geometry optimization of the complexes was performed with BP86 exchange-correlation functional including Becke's exchange part [26] and Perdew's gradient corrected correlation part [27]. All calculations were done with the PCGAMESS v.7.01. build 3666 program [28]. Energies of singlet and triplet states within the broken-symmetry approach and distribution of spin density at the found geometry were calculated using hybrid B3LYP functional, consisting of non-local hybrid exchange functional as defined by Becke's three parameter equation [29] and the non-local Lee–Yang–Parr correlation functional [30]. The Gaussian '03 was employed for these calculations [31]. The basis set used was 6-31G(d). Presentation graphics and visualization of the quantum-chemical modelling results were performed with the help of the Chemcraft program [32].

3. Results and discussion

3.1. *Structure of the 2,6-diformyl-4-*tert*-butylphenol-*bis*-(1′-phthalazinylhydrazone) (H_3L)*

The structure of the novel Robson-type ligand H_3L was determined based on the elemental analysis (see table 1), ^{1}H NMR and IR spectral data and comparison of the spectra with theoretically calculated ones within the DFT approach.

Tautomeric properties of the ligand are important in determining the structure obtained. Hydrazone **1** contains nine donor atoms and three mobile protons, giving rise to many possible tautomeric forms. The most probable tautomers were modelled at a BP86/6-31G(d) level to find the most stable. The preferred conformers of these tautomers are shown in figure 1; calculated total energy and energy relative to the most stable (**1a**) are listed in table 2.

Calculations show the potential energy surface for OH proton transfer between phenolic oxygen and azomethine nitrogen has only one minimum, corresponding to phenolic tautomer form. When starting geometry optimization from the quinonoid structure the result is always phenolic tautomer, transfer of the proton from nitrogen to oxygen atom takes place without energy barrier.

The most destabilized isomers are of quinonoid form (**1d**, **1e**), with non-symmetrically shifted protons. The most stable are phenolic tautomers, involving distribution of the remaining two protons over azomethine nitrogen and phthalazine nitrogen in position 3 of the ring (**1a**, **1b**, **1c**). The lowest energy is calculated for **1a** isomer, which is

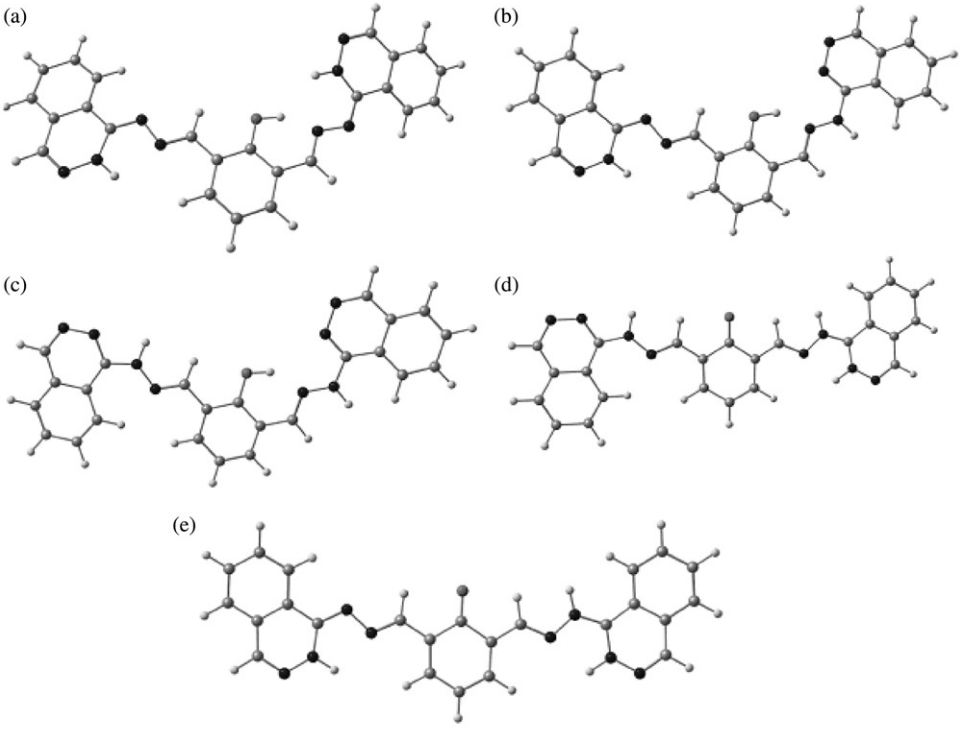

Figure 1. Tautomeric forms of hydrazone **1**.

Table 2. Total energy (Hartree) and relative stability of the tautomeric forms of hydrazone **1** according to the most stable one (1a, kcal mol^{-1}).

Isomer	E (Hartree)	ΔE (kcal mol^{-1})
1a	−1438, 547,092	0.0
1b	−1438, 528,121	11.9
1c	−1438, 517,452	18.6
1d	−1438, 499,888	29.6
1e	−1438, 508,956	23.9

ca 11 kcal mol^{-1} lower in energy than the next stable isomer, **1b**. Three hydrogen bonds stabilize the planar structure of the molecule; the most intensive of them is the bond OH$\cdots$N$_{az}$ (see figure 1, **1a**). Right (on the figure) phthalazine moiety of the molecule is twisted along N–N bond by ca 16 degrees to minimize OH$\cdots$HN repulsion.

This result is supported by ^{1}H NMR spectra of **1**. In low field region, there are two groups of signals with 2 : 1 intensity ratio, showing existence of symmetrical tautomeric forms of side chains of the ligand and phenolic group. Two-proton signal (12.1 ppm) is shifted significantly downfield relative to two one-proton signals (11.0 ppm). Also, tautomeric shift of the protons from hydrazine nitrogen to phthalazine heterocyclic

Table 3. Experimental and calculated (for isomer 1a) IR spectral data of hydrazone **1**.

	Calculated		Experimental
Assignment	Frequency (cm^{-1})	Intensity ($kM\,mol^{-1}$)	Frequency (cm^{-1}) (intensity*)
ν(NH)	3525	41	3410(m)
ν(NH)	3463	52	3340(m)
ν_s(C_{ar}–H, phthal)	3147	7	
ν_s(C_{ar}–H, phthal)	3144	12	
ν_s(C_{ar}–H, phen)	3140	11	
ν_{as}(C_{ar}–H, phthal)	3133	11	2800–3000
ν_{as}(C_{ar}–H, phthal)	3131	12	(broad vs)
ν(C–H, azomethine)	3053, 3026	13, 16	
ν(OH)	2807	1113	ca 3000(broad)
δ(OH)	1640	59	1630(vs)
ν(C=N)	1611, 1607	316, 465	1620(s)
ν(C=C, ar)	1604, 1600	21, 246	1600(s)
ν(C=N, phthal)	1588, 1580, 1576	26, 83, 268	1580(m)
ν(C=C, C=N, phthal)	1551, 1530, 1516	183, 113, 350	1545(m)
ν(C=C, phthal)	1458, 1454	26, 14	1480(s)
ν(C=C, phthal)	1449, 1446	20	1455(s)
ν(C–O, phen)	1421	85	1440(s)
	1382, 1376	90	1390(m)
	1363, 1364	23, 31	1350(m)
ν(C=N, phthal)	1309, 1322	16, 179	1305(m)
	1301	90	1280(w)
ν(C–O, phen)	1264	30	1265(m)
	1232, 1234, 1236	34, 68, 52	1230(w)
ν(C–N, phthal)	1223, 1224	18, 12	1225(w)

*Intensities are denoted as follows: vs-very strong, s-strong, m-medium, w-weak.

nitrogen is proved by X-ray analysis for hydrazone of pyruvaldehyde with 1-hydrazinophthalazine [33].

Absence of quinonoid isomer in the crystal phase is confirmed by IR spectra since characteristic stretching vibrations of C=O double bond are not observed in the region of $1680\,cm^{-1}$.

For the **1a** tautomer, molecular vibration spectra were calculated employing harmonic approximation. Experimental, calculated spectra and assignments of the bands in IR spectra from theoretical results are listed in table 3.

Two signals at 3340 and $3410\,cm^{-1}$ are assigned to N_{pht}–H bond stretching that confirms the non-symmetric tautomeric form of hydrazone **1** in crystal state. ν(OH) is observed as a very broad low maxima at ca $3000\,cm^{-1}$ shifted to lower frequencies due to involvement in very strong intramolecular hydrogen bonds with an azomethine nitrogen. This bond is also responsible for observation of δ(OH) vibration band at $1630\,cm^{-1}$.

3.2. *Composition of the complexes*

The most significant factor influencing the composition and structure of the synthesized complexes is the metal salt used for complex formation. Composition of **2**, obtained by reaction of *bis*-hydrazone (**1**) with copper(II) acetate corresponds to formula

$[Cu_2L(\mu\text{-}OCH_3)] \cdot CH_3OH$, where L^{3-} is a triply deprotonated form of *bis*-hydrazone (see table 1). Negligible conductance of the DMF solution of **2** supports formation of neutral complex. Complexes formed by reaction of *bis*-hydrazone (**1**) with copper(II) halides, **3** and **4**, have common formula $[Cu_2H_2LX_3] \cdot (CH_3OH)$ (X = Cl, Br); reaction with oxovanadium(IV) chloride leads to formation of the complex $[(VO)_2H_2L(\mu\text{-}Cl)]Cl_2 \cdot (CH_3OH)$. Conductivity measurements of complex solutions in DMF show that non-bridging halogen ions for **3**–**5** are bonded to the molecule in a different manner. Molar conductances of solutions **3** and **4** fall in the expected range for non-electrolytes, indicating that the halide ions are located inside the coordination sphere of copper. Molar conductivity of **5** falls in the expectation range for 2 : 1 electrolytes [34], supporting formation of cationic complexes with chloride outside the metal coordination sphere.

3.3. *IR spectra*

Assignment of the absorption bands in the infrared spectra of the complexes was performed according to literature [23, 35] and the results of quantum chemical modelling of H_3L (see table 3). In the spectra of all studied complexes broad band at ca 3460 cm^{-1} is observed due to crystallization methanol. Selected vibration bands are listed in table 4.

Infrared spectra of the complexes features the following details: in spectra of **2** the band corresponding to stretching vibrations of phenoxide OH group and hydrazone NH groups are absent, showing coordination of the ligand as triply negative ion (see table 4). High degree of deprotonation in reaction with copper(II) acetate is observed due to deprotonation activity of acetate in non-aqueous solution and high mobility of the protons in the ligand.

OH bond stretching vibrations also disappear in IR spectra of **3**–**5** as compared to IR spectra of the ligand. But, the NH stretching vibration in **3**–**5** indicates coordination of the ligand in mono deprotonated form H_2L^-. Presence of metal ion shifts tautomeric equilibrium from isomer **1a** towards **1c**.

Stretching vibration of azomethine observed at 1620 cm^{-1} in hydrazone **1** shifts to lower frequencies in complexes **2**–**5** due to formation of the bond between metal ion and azomethine nitrogen. Stretching vibrations of the phthalazine rings C=N bond shifts to higher frequencies, indicating strengthening of double character of these bonds upon coordination.

Thus, based on the elemental analysis, conductivity measurements and IR spectroscopy data, the compounds studied can be ascribed by the structures shown in figure 2.

Table 4. Experimental IR spectral data of **1**–**5** (cm^{-1}).

Compound	ν(OH)	ν(NH)	ν(C–O) (phenolic)	ν(C–O) (phenolic)	ν(C=N) (azomethine)	ν(C=N) (phthalazine)
1	ca 3000	3410, 3340	1440	1265	1620	1580
2	–	–	1440	1295	1615	1595
3	–	3320	1405	1290	1610	1590
4	–	3310	1400	1295	1610	1590
5	–	3310	1420	1300	1605	1595

3.4. *ESR spectra*

The ESR spectra of the polycrystalline copper complexes **2**–**4** at room temperature is typical for an isotropic local molecular environment ($g_{iso} = 2.10$). The broad signal at 1400 G was assigned to the $\Delta M_s = \pm 2$ transition arising from coupling between two $S = 1/2$ copper ions. Interaction between equivalent ions is responsible for the quite sharp absorption line in the ESR spectrum [36].

3.5. *Magnetic properties*

Magnetic data are summarized in table 5. Temperature dependence of magnetic susceptibility for all complexes reveals the existence of antiferromagnetic exchange.

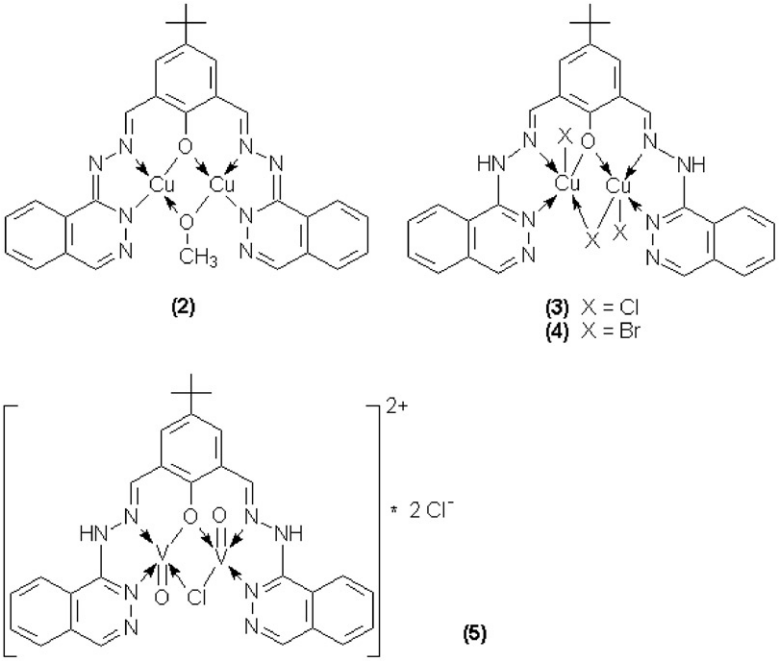

Figure 2. Structure of the complexes **2**–**5**.

Table 5. Magnetic data of **2**–**5**.

Compound	T (K)	μ_{ef} (B.M.)*	$-2J$ (cm^{-1})	g	ρ
2	296	0.62	~700	–	–
	77.4	Diamagnetic			
3	295	1.77	73	2.11	0.01
	77.4	1.41			
4	298	1.80	50	2.12	0.01
	77.4	1.58			
5	298	1.49	190	2.00	0.03
	77.4	0.68			

*The effective magnetic moments are calculated per one metal ion.

The magnetic data were interpreted in terms of HDVV (Heisenberg–Dirac–Van–Vleck) spin-Hamiltonian which implies an isotropic interaction between paramagnetic centers described through an exchange constant $2J$ in the form:

$$H = -2J \cdot \hat{S}_a \cdot \hat{S}_b. \tag{1}$$

Temperature dependence of magnetic susceptibility data of copper(II) and oxovanadium(IV) complexes were fitted with the Bleaney–Bowers equation modified to take into account the paramagnetic impurities (equation 1) [37].

$$\chi'_{\mathrm{m}} = \frac{2N_{\mathrm{A}}g^2\beta^2}{3kT}\left[(1-\rho)\left[1+\frac{1}{3}\exp\left(\frac{-2J}{kT}\right)\right]^{-1} + \rho \cdot S(S+1)\right] + N_\alpha, \tag{2}$$

where $\rho =$ molar fraction of paramagnetic admixture, S is total spin of paramagnetic admixture, N_{A}, g, β, k have their usual meaning.

Magnetic moment of **2** at room temperature is as low as 0.62 B.M. (calculated per one copper ion) and becomes zero when cooled to 240 K; value of the exchange parameter $2J$ in this case can be evaluated as $-700\,\mathrm{cm}^{-1}$. This value is in good agreement with previous results [12, 23, 38–40], showing that for copper(II) complexes with triply deprotonated Robson-type ligands with analogous structure and μ-alkoxo exogenous bridges, exchange interaction is highly antiferromagnetic due to the structure of the complexes where exchange fragment

is completely planar and lies in the plane of the whole molecule, which is ensured by extensive π-conjugation. For a number of complexes this is supported by both magnetic data and X-ray analysis [2, 13, 14, 41–43]. Since magnetic exchange in analogous binuclear complexes tends to be dependent on the electronegativity of non-bridging donor atoms, for complexes of *bis*-hetarylhydrazones antiferromagnetic coupling appears to be stronger than for *bis*-acylhydrazones of 2,6-diformyl-4-R-phenols for which typical exchange integral $2J$ values fall in the range -250–$400\,\mathrm{cm}^{-1}$ [18–20].

For **3**–**5** magnetic moments significantly decrease when cooling to liquid nitrogen temperatures, revealing the existence of antiferromagnetic exchange interaction; $2J$ values calculated are -73, -50 and $-190\,\mathrm{cm}^{-1}$.

Considerable decrease of exchange coupling from (μ-OCH_3) bridge in **2** to (μ-Cl) bridge in **3** is explained as follows. Since interatomic distance Cu–Cl is approx. 0.4 Å longer than Cu–OCH_3, such substitution leads to significant changes in geometry of the coordination units. Bond angle Cu–X–Cu decreases from ca 100 in methoxy bridged complexes to ca 90 for chloride bridge. The planar structure of the complex is distorted by displacement of the copper ions out of the molecule plane. This distortion leads to preferable coordination of the fifth ligand (counter-ion) and formation of pentacoordinated structure of each copper center [18–20, 42, 44, 45]. Both factors result in less overlap of magnetic orbitals of paramagnetic metal centers.

Further weakening of the antiferromagnetic interaction in binuclear copper(II) complexes with bromide bridging anion relative to the chloride-containing complexes

with analogous structure is rather common and traditionally explained by even more distortion of the exchange fragment caused by more bulky bromide ion [18–20, 44, 45].

The value of exchange parameter, obtained for **5** ($-190\,cm^{-1}$), is typical for oxovanadium(IV) binuclear complexes with four-membered exchange fragment. Exchange in these complexes is rather insensitive to variation in ligand environment and bridging groups and usually lies in the range -150–$300\,cm^{-1}$ [46–48]. This indicates that contribution of the superexchange pathway in the magnetic interaction of the paramagnetic centers in oxovanadium(IV) binuclear complexes is small compared to direct interaction.

3.6. *DFT study of complexes 2–5*

3.6.1. Theoretical background of the magnetic exchange quantum-chemical calculations. Exchange interaction between two paramagnetic centers A and B with local spins $s_A = s_B = 1/2$ is expressed as an energy difference between resulting total low-spin (LS, $S = 0$ – the first singlet) and high-spin (HS, $S = 1$ – the lowest triplet) states:

$$-2J = E(S = 0) - E(S = 1). \tag{3}$$

In case of near degenerate orbital energies of the interacting electrons and weak interaction between the centers, proper description of the LS (singlet) state cannot be achieved within single Slater type determinant (SD) wavefunction. The reason is existence of several low lying singlet states with little energy differences between them (first three states on the scheme below) resulting in strong correlation energy.

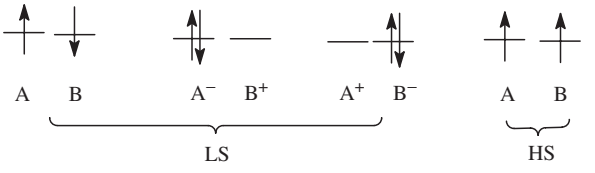

Contrary, HS state of binuclear transition metal complexes could be rather satisfactorily described by SD wavefunction (fourth state on the scheme).

Thus, direct evaluation of the $2J$ value as the energy difference between pure singlet and triplet states would give reasonable results only within carefully constructed post-HF methods. Time-consuming complete active space SCF (CASSCF) and MP2 corrected CASSCF-CASPT2 methods are widely and effectively used for theoretical magnetic exchange prediction. Of course, only small to medium size complexes can be treated within these approaches.

An alternative approximate method for $2J$ calculation was proposed by Ginsberg, Noodleman, Yamaguchi and others and is called broken symmetry approach [49, 50]. They showed that the energy gap between pure spin states (equation 3) can be approximated by the energy difference between so called broken symmetry state (BS) and triplet state which are determined as SD unrestricted wavefunctions (UHF or UDFT).

$$-2J = \frac{2(E_{BS} - E_T)}{1 + s_{AB}^2}. \tag{4}$$

Here s^2_{AB} denotes overlap integral between two magnetic orbitals localized on centers A and B. Broken-symmetry solution for singlet state is obtained by allowing the electron distribution symmetry to be lower than the actual spatial symmetry of the molecule. Two polar regimes are used in practical calculations—'strong delocalized limit' ($s^2_{AB} = 1$) and 'strong localized limit' ($s^2_{AB} = 0$) along with direct evaluation of the overlap integral between magnetic orbitals [51].

3.6.2. Structure of 2–5. Calculated values of singlet-triplet state energy splitting are very sensitive towards variation of the molecular geometry. That is why theoretical calculations of magnetic exchange were performed employing experimental atomic coordinates determined from single crystal X-ray data. In the present study we used optimized geometrical structure of the model complexes employing GGA DFT approximation with BP86 correlation-exchange functional which was recently shown to behave somewhat better than widely used hybrid B3LYP functional for reproduction of the transition metal complex geometry [52].

Singlet and triplet states, determining the intensity of the magnetic exchange interaction, are long lived thermally populated states and position of the nuclei in these states should be considered different. Hence, equilibrium geometry must be separately found for each electronic state. For rather large systems, such as those considered in the current study, geometry optimization with the multiconfiguration wavefunction is time consuming. But, from the closeness of the energies of the states one can conclude that difference in relaxed coordinates must not be expected to be significant. Taking into consideration complexity of the low spin state wavefunction, the best way to obtain good approximation to the geometry of the complex is optimization of the HS state, which can be reasonably described by SD wavefunction within unrestricted SCF or DFT approach.

Geometry of all model complexes was optimized at the UBP86/6-31G(d) level in the lowest triplet state. Selected bond lengths and angles are gathered in table 6. Molecular models are depicted in figure 3.

Ligand is coordinated through two phthalazine (N_{pht}) and two azomethine (N_{az}) nitrogen atoms and phenoxide oxygen (O_{ph}). In all complexes four-member exchange

Table 6. Selected bond lengths (Å) and angles (°) within metal ion coordination sphere of **2**–**5** calculated at UBP86/6-31G(d) level of theory for HS state.

Parameter	**2**	**3**	**4**	**5**
N_{pht}–M	1.975	1.945	1.949	2.044
N_{az}–M	1.991	2.021	2.021	2.074
O_{ph}–M	2.005	2.004	2.007	2.047
X_{br}–M	1.912	2.359	2.466	2.362
$X_{non\text{-}br}$–M	–	2.273	2.420	–
M···M	2.995	3.270	3.309	3.311
M–O_{ph}–M	96.8	109.4	111.0	108.0
O_{ph}–M–X	80.0	81.4	82.3	81.5
M–X–M	103.2	87.7	84.3	89.0

fragment

(X = Cl, Br or OCH_3) is formed.

The optimal conformer of **2** corresponds to near-to-planar configuration with C_s symmetry (mirror plane is the plane of the molecule). The C–O bond and one of the C–H bonds of the bridging methoxide group are located in the symmetry plane. Triple deprotonation of the ligand results in shorter Cu–N_{az} bonds compared with **3** and **4** with monodeprotonation of ligand. Distance between copper and phenoxide oxygen is practically the same in **2**–**4**. Distance between copper(II) centers is the shortest for **2** (2.995 Å) due to the small size of methoxide bridge – bond length Cu–OCH_3 is 1.912 Å.

Copper(II) complexes **3** and **4** have rather similar structure with very close to C_2 symmetry (see figure 3b). Two pentacoordinate copper ions have distorted trigonal bipyramidal environment, with common axial donor atom, phenoxide oxygen. Opposite axial position is occupied by phthalazine nitrogen. Angles between axial bonds are equal to 156 degrees for **3** and 157 degrees for **4**. Two halides (common for both polyhedron bridging halide and one of the exocyclic coordinated to the copper center) and azomethine nitrogen lie in an approximate equatorial plane. Five-member chelate cycles of the complexes formed by phthalazine and azomethine donor atoms are practically planar, whereas six-member chelate cycles are heavily distorted mainly by bending of the chelate plane along O···N line by ca 36 degrees.

In both complexes four-member exchange fragment is virtually planar and twisted with respect to the molecular plane along axes connecting bridging atoms by 37 and 38 degrees for chloride and bromide bridges, respectively. Larger radius of bromide anion (and resulting longer copper-bridging bromide distances) is responsible for redistribution of angles in exchange fragment compared to **3**: Cu–O–Cu, O–M–X angle are enlarged, but Cu–Br–Cu angle is diminished (84.3 for **4** compared with 87.7 for **3**). Cu···Cu distance in **4** is 3.309 Å, 0.039 Å longer than in **3**.

Optimal geometry of the oxovanadium(IV) complex, **5**, is also of C_2 symmetry, where symmetry axis goes through the bridging Cl, O atoms of the exchange fragment. Contrary to **3** and **4** with trigonal pyramidal structure metal ion coordination

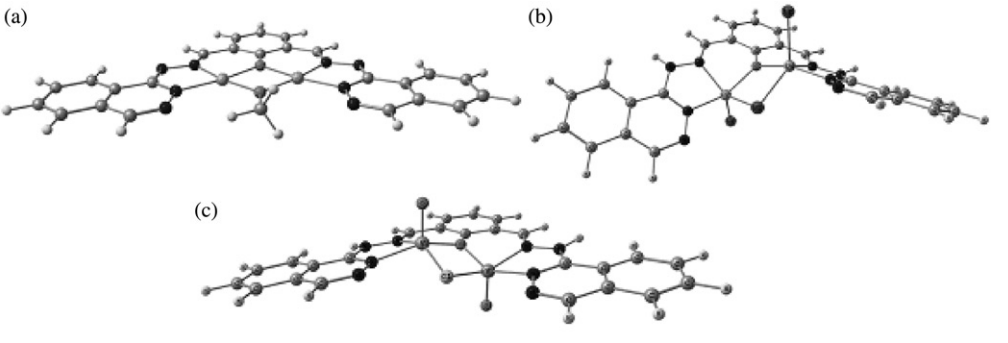

Figure 3. Magnetic orbitals of copper (II) complex **2** (a) and oxovandium (IV) complex **5** (b).

Table 7. Mulliken atomic spin densities within the nearest coordination sphere of the metal ions in high-spin (HS) and low-spin (LS) states for **2**–**5**.

	2		**3**		**4**		**5**	
Atom	LS	HS	LS	HS	LS	HS	LS	HS
M_1	−0.650	0.669	−0.724	0.729	−0.694	0.699	−1.163	1.172
N_{az1}	−0.093	0.086	−0.043	0.052	−0.042	0.051	0.012	−0.012
N_{pht1}	−0.095	0.086	−0.080	0.081	−0.084	0.086	0.018	−0.018
X_1	–	–	−0.050	0.052	−0.059	0.063	0.162	−0.016
O	0.000	0.094	0.000	0.080	0.000	0.085	0.000	−0.001
X	0.001	0.116	0.000	0.093	0.000	0.120	0.000	−0.010
M_2	0.650	0.663	0.724	0.729	0.694	0.699	1.162	1.172
N_{az2}	0.093	0.093	0.043	0.052	0.042	0.051	−0.012	−0.012
N_{pht2}	0.095	0.100	0.079	0.081	0.084	0.086	−0.018	−0.018
X_2	–	–	0.051	0.052	0.059	0.063	−0.162	−0.162

polyhedron in **5** is square pyramidal with oxovanadium oxygen in axial position. Exchange fragment is totally planar and is twisted along the C–O bond by 23 degrees relative to the plane of the phenolic fragment. Oxovanadium groups are shifted on the opposite sides from the molecular plane. Compared to **2**–**4** more long bond lengths in the coordination sphere of the vanadium(IV) ion are observed proving more localized d-electrons in **5**. Distance between vanadium centers – 3.311 Å is the longest among the series studied.

Distribution of atomic Mulliken spin density in HS and LS states of **2**–**5** is shown in table 7. In singlet states of the complexes α- and β-spin densities are spatially separated between metal ions. Absolute values of spin densities on atoms of the same complex in different electronic states are very close to each other. Difference of the spin density values on metal centers correlates well with the $2J$ values; for complexes with small exchange (**3**, **4**) it is as low as 0.005, for **5** – 0.090 and for the complex **2** with the strongest exchange – 0.019. Expectation value of $\mathbf{S^2}$ operator ($\langle \mathbf{S^2} \rangle$, see table 7) of BS states are close to one indicating strong admixture of states with higher multiplicity. It can be mentioned that for complexes with small $2J$ values **3**, **4** and **5** deviation from unity is small, while it is more pronounced for **2** with strong antiferromagnetic coupling. HS state $\langle \mathbf{S^2} \rangle$ values are close to 2, proving that triplet state is sufficiently well described by SD wavefunction.

There is a marked difference in distribution of the spin density in copper(II) and oxovanadium(IV) complexes. Primarily, in copper complexes delocalization of spin density is significant, but in oxovanadium complex it is located practically 100% on the VO fragment. Second, bridging atoms in copper complexes gain significant spin density in the triplet state (0.093 for **3**, 0.120 for **4** and 0.116 for **2**) contrary to one order of magnitude less 0.010 value for oxovanadium complex. Consequently, superexchange mechanism through bridging atoms prevails in paramagnetic centers interaction for copper binuclear complexes, whereas direct d–AO exchange is observed in **5**. These results are in line with earlier hypothesis that exchange between oxovanadium(IV) ions occur through direct, not superexchange pathway [18, 41, 42].

In copper(II) complexes bridging X groups bear more spin density than the phenoxide oxygen, and thus pathway of superexchange through X bridge is more significant than through phenoxide bridge.

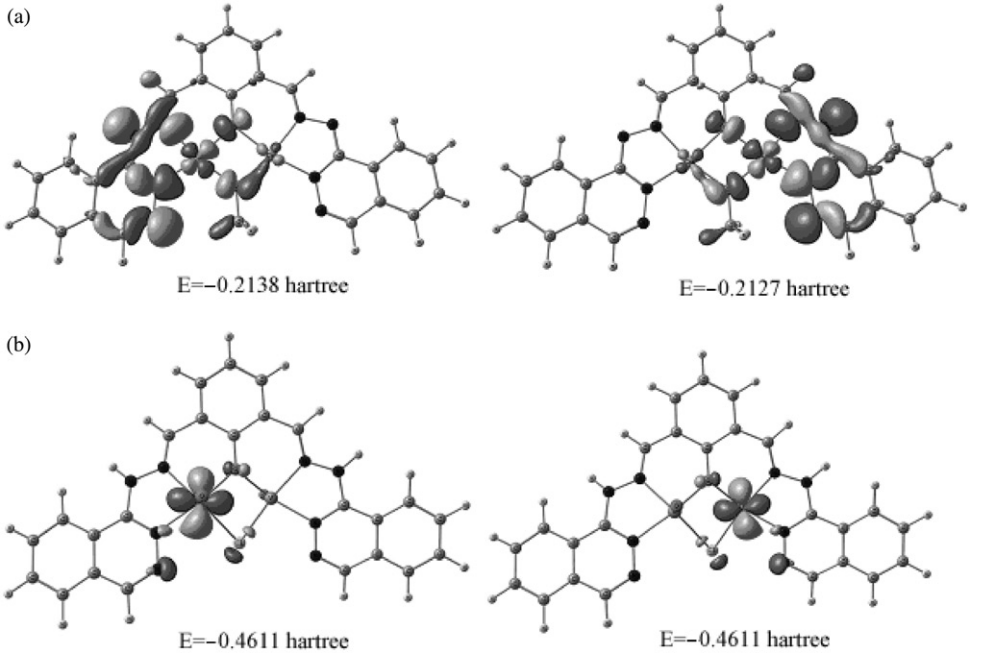

Figure 4. Equilibrium conformation of the copper (II) complexes **2** (a), **3** (b) and oxovanadium (IV) complexes (c).

Magnetically active, singly occupied, molecular orbitals (SOMO's), which are responsible for spin density distribution in all of the complexes, are not the frontier orbitals of the complexes and lie beneath the highest occupied MO (HOMO). Figure 4 presents α- (left) and β-spin (right) magnetic SOMOs of low spin state for copper(II) **2** (a) and oxovanadium(IV) complex **5** (b) with their energies. For copper complexes **2**–**4** they are extensively delocalized over the nearest to the metal atoms of the ligand with large contribution of the bridging atoms (see as example figure 4a for complex **2**). Contrary, in oxovanadium(IV) complex **5** magnetic MO's are strongly localized and are practically pure metal d–AO combinations with very small participation of ligand AOs (figure 4b). For vanadium complex magnetic SOMOs are significantly lower in energy compared with **2**–**4**.

Calculated at UB3LYP/6-31G(d) energies of the LS, HS states and $2J$ values are collected in table 8. Since in copper complexes magnetic MOs are significantly delocalized over bridging and non-bridging donor atoms the strong delocalized limit was used to obtain, calculated with equation (4), singlet–triplet splitting for **2**–**4**. In case of **5**, from the shape of the magnetic SOMOs one can expect small value of orbital overlap due to their strong localization on vanadium ions and rather long interatomic V $\cdots$ V distances and thus, strong localization limit is more justified.

Excellent correlation is observed between calculated and experimental exchange parameter values in case of **3**, **4** and **5**, supporting the right choice of the approximation used in these cases. For **2** with methoxide bridging group the calculated energy gap between LS state and HS states is lower than experimentally obtained $2J$ value. Deviation of the calculated values of the energy gap between singlet and triplet states

Table 8. Energies of the lowest singlet (LS) and triplet (HS) states, corresponding expectation values of total spin square operator $\langle \mathbf{S^2} \rangle$ (in brackets) and $2J$ values calculated at UB3LYP/6-31G(d) level of theory.

Complex	$E(S=0)$, Hartree	$E(S=1)$, Hartree	$2J$ (cm^{-1})		
			Exp.	Calcd[a]	Calcd[b]
2	−4832.6225427 (0.9597)	−4832.6199435 (2.0048)	−700	−570	
3	−6099.3249038 (0.9964)	−6099.3246210 (2.0079)	−70	−62	
4	−12433.9146997 (0.9959)	−12433.9144587 (2.0085)	−50	−53	
5	−3936.3632949 (1.0202)	−3936.3628074 (2.0286)	−190		−214

[a]Strong delocalization limit is used in equation (4).
[b]Strong localization limit is used in equation (4).

towards underestimating of antiferromagnetic exchange for **2** (with higher antiferromagnetic exchange interaction compared to **3** and **4**) can be attributed to neglecting of geometry relaxation between singlet and triplet states. For larger $2J$ values the difference in geometry of these states is expected to be considerable. When using X-ray crystal structures of the complexes for calculations of exchange parameter this effect is compensated to some extent, because experimental geometry is an average mix of the geometries of thermally populated low- and high-spin states of the molecule.

In any case the calculated $2J$ values are in reasonable agreement with experimental values.

4. Conclusion

Four binuclear complexes: $[Cu_2L(\mu\text{-}OCH_3)] \cdot CH_3OH$, $[Cu_2H_2L(\mu\text{-}Cl)Cl_2] \cdot (CH_3OH)$, $[Cu_2H_2L(\mu\text{-}Br)Br_2] \cdot (CH_3OH)$, $[(VO)_2H_2L(\mu\text{-}Cl)]Cl_2 \cdot (CH_3OH)$ of the Robson-type binucleating ligand (2,6-diformyl-4-*tert*-butylphenol-*bis*-(1′-phthalazinylhydrazone)) were synthesized and their physical–chemical properties studied. Significant influence on the structure of the synthesized compounds is made by metal salt used for complex formation, which determines the exogenous bridging group and the degree of the ligand deprotonation. Both features are important for magnetic exchange interaction between paramagnetic centers. In all complexes exchange coupling is observed, exchange parameter values are −700, −73, −50 and $-190\,cm^{-1}$. DFT calculations at UB3LYP/6-31G(d) level of theory were used to study electronic structure of the complexes. Mechanism of magnetic interaction is direct exchange in case of oxovanadium(IV) complex and superexchange via bridging donor atoms in case of copper(II) complexes. Calculated within the broken symmetry approach, values of singlet–triplet state splitting (−570, −62, −53, $-214\,cm^{-1}$, correspondingly) closely approximate experimental data.

Acknowledgments

This research was funded by Russia's Presidential program for state support of the young scientists (grant No. MK-1249.2006.3). Authors of the article thank G. Zhurko

for granting Chemcraft visualization software widely used for data processing and presentation graphics within this research.

References

[1] H. Okawa, S. Kida, Y. Mutto, T. Tokii. *Bull. Chem. Soc. Jpn*, **45**, 2480 (1972).
[2] M. Sakamoto, S. Itose, T. Ishimori, N. Matsumoto, H. Okawa, S. Kida. *J. Chem. Soc., Dalton Trans.*, 2083 (1989).
[3] E.E. Eduok, C.J. O'Connor. *Inorg. Chim. Acta*, **88**, 229 (1984).
[4] M.L. Boilot, O. Kahn, C.J. O'Connor, J. Gouteron, S. Jeannien, Y. Jeannien. *J. Chem. Soc., Chem. Commun.*, 178 (1985).
[5] T. Mallah, M.L. Boilot, O. Kahn, J. Gouteron, S. Jeannien, Y. Jeannien. *Inorg. Chem.*, **25**, 3058 (1986).
[6] R.L. Carlin, R. Block. *Proc. Indian Acad. Sci. (Chem. Sci.)*, **98**, 1–2, 79 (1987).
[7] O. Kahn. *Inorg. Chim. Acta*, **62**, 3 (1982).
[8] R. Robson. *Aust. J. Chem.*, **23**, 2217 (1970).
[9] R. Robson. *Inorg. Nucl. Chem. Lett.*, **6**, 125 (1970).
[10] R. Robson. *Inorg. Chim. Acta*, **57**, 71 (1982).
[11] G. Paolucci, P.A. Vigato, G. Rosseto, V. Casellato. *Inorg. Chim. Acta*, **65**, L71 (1982).
[12] S.I. Levchenkov, V.A. Kogan, V.V. Lukov. *Russ. J. Inorg. Chem.*, **38**, 12, 1992 (1993).
[13] P. Cheng, D. Liao, S. Yan, Z. Jiang, G. Wang, X. Yao, H. Wang. *Inorg. Chim. Acta*, **248**, 135 (1996).
[14] P. Cheng, D. Liao, S. Yan, J. Cui, Z. Jiang, G. Wang, X. Yao, H. Wang. *Helv. Chim. Acta*, **80**, 213 (1997).
[15] C.J. O'Connor, D.A. Firmin, A.K. Pant, B. Ram Babu, E.D. Stevens. *Inorg. Chim. Acta*, **25**, 2300 (1986).
[16] T. Mallah, M.L. Boilot, O. Kahn, C.J. O'Connor, J. Gouteron, S. Jeannien, Y. Jeannien. *Inorg. Chem.*, **26**, 1375 (1987).
[17] T.N. Sorrell, C.J. O'Connor, O.P. Anderson, J.H. Reibenspies. *J. Am. Chem. Soc.*, **107**, 4199 (1985).
[18] O. Kahn. *Theoret. Approach*, 89 (1987).
[19] V.A. Kogan, V.V. Lukov. *Russ. J. Coord. Chem.*, **23**, 1, 18 (1997).
[20] V.A. Kogan, V.V. Lukov. *Russ. J. Coord. Chem.*, **24**, 3, 189 (1998).
[21] S.M. Annigeri, A.D. Naik, U.B. Gangadharmath, V.K. Revankar, V.B. Mahale. *Transition Met. Chem.*, **27**, 3, 316 (2002).
[22] A.D. Naik, S.M. Annigeri, U.B. Gangadharmath, V.K. Revankar, V.B. Mahale. *Transition Met. Chem.*, **27**, 3, 333 (2002).
[23] S.I. Levchenkov, V.V. Lukov, V.A. Kogan, L.D. Popov, I.N. Shcherbakov. *Russ. J. Inorg. Chem.*, **38**, 10, 1687 (1993).
[24] R.S. Drago, M.J. Desmond, B.B. Corden, K.A. Miller. *J. Am. Chem. Soc.*, **105**, 2287 (1983).
[25] B. Bleaney, K.D. Bowers. *Proc. R. Soc. London, Ser. A*, **214**, 451 (1952).
[26] A.D. Becke. *Phys. Rev. A*, **38**, 3098 (1988).
[27] J.P. Perdew. *Phys. Rev. B*, **33**, 8822 (1986).
[28] A.A. Granovsky. PC GAMESS version 7.0, http://classic.chem.msu.su/gran/gamess/index.html
[29] A.D. Becke. *J. Chem. Phys.*, **98**, 5648 (1993).
[30] C. Lee, W. Yang, R.G. Parr. *Phys. Rev. B*, **37**, 785 (1988).
[31] M.J. Frisch, G.W. Trucks, H.B. Schlegel, G.E. Scuseria, M.A. Robb, J.R. Cheeseman, J.A. Montgomery Jr, T. Vreven, K.N. Kudin, J.C. Burant, J.M. Millam, S.S. Iyengar, J. Tomasi, V. Barone, B. Mennucci, M. Cossi, G. Scalmani, N. Rega, G.A. Petersson, H. Nakatsuji, M. Hada, M. Ehara, K. Toyota, R. Fukuda, J. Hasegawa, M. Ishida, T. Nakajima, Y. Honda, O. Kitao, H. Nakai, M. Klene, X. Li, J.E. Knox, H.P. Hratchian, J.B. Cross, C. Adamo, J. Jaramillo, R. Gomperts, R.E. Stratmann, O. Yazyev, A.J. Austin, R. Cammi, C. Pomelli, J.W. Ochterski, P.Y. Ayala, K. Morokuma, G.A. Voth, P. Salvador, J.J. Dannenberg, V.G. Zakrzewski, S. Dapprich, A.D. Daniels, M.C. Strain, O. Farkas, D.K. Malick, A.D. Rabuck, K. Raghavachari, J.B. Foresman, J.V. Ortiz, Q. Cui, A.G. Baboul, S. Clifford, J. Cioslowski, B.B. Stefanov, G. Liu, A. Liashenko, P. Piskorz, I. Komaromi, R.L. Martin, D.J. Fox, T. Keith, M.A. Al-Laham, C.Y. Peng, A. Nanayakkara, M. Challacombe, P.M.W. Gill, B. Johnson, W. Chen, M.W. Wong, C. Gonzalez, J.A. Pople. *Gaussian 03, Revision A.1*, Gaussian, Inc., Pittsburgh PA (2003).
[32] G.A. Zhurko. Chemcraft ver. 1.5 trial, build 266. http://www.chemcraftprog.com
[33] G. Giorgi, F. Ponticelli, L. Savini, L. Chiasserini, C. Pellerano. *J. Chem. Soc., Perkin Trans.*, **2**, 2259 (2000).
[34] W.J. Geary. *Coord. Chem. Rev.*, **7**, 81 (1971).

[35] G. Paolucci, S. Stelluto, S. Sitran, D. Ajo, F. Benetollo, A. Polo, G. Bombieri. *Inorg. Chim. Acta*, **193**, 57 (1992).
[36] I.M. Procter, B.J. Hathaway, D. Nicholls. *J. Chem. Soc. (A)*, 1678 (1968).
[37] E.A. Boudreaux, L.N. Mulay. *Theory and Applications of Molecular Paramagnetism*, p. 491, Wiley, New York (1976).
[38] A.D. Naik, V.K. Revankar. *Ind. J. Chem.*, **43A**, 1447 (2004).
[39] V.V. Lukov, S.I. Levchenkov, V.A. Kogan. *Russ. J. Coord. Chem.*, **25**, 1, 51 (1999).
[40] V.V. Lukov, S.I. Levchenkov, S.V. Posokhova, I.N. Shcherbakov, V.A. Kogan. *Russ. J. Coord. Chem.*, **28**, 3, 234 (2002).
[41] A.S. Antsyshkina, M.A. Porai-Koshits, G.G. Sadikov, V.V. Lukov, V.A. Kogan, S.I. Levchenkov. *Russ. J. Inorg. Chem.*, **39**, 6, 905 (1993).
[42] F.K. Zhovmir, Yu.A. Simonov, V.V. Zelentsov, N.V. Gerbeleu, M.D. Revenko, A.K. Stroesku, A.N. Sobolev. *Russ. J. Inorg. Chem.*, **33**, 8, 2180 (1986).
[43] P. Iliopoulos, K.S. Murrey, R. Robson, J. Wilson, G.A. Williams. *J. Chem. Soc., Dalton Trans.*, 1585 (1987).
[44] C.J. Cairns, D.H. Bush. *Coord. Chem. Rev.*, **69**, 1 (1986).
[45] O. Kahn. *Inorg. Chim. Acta*, **62**, 3 (1982).
[46] H. Okawa, I. Ando, S. Rida. *Bull. Chem. Soc. Jpn*, **44**, 12, 3041 (1974).
[47] S. Mukherjee, T. Weyhermüller, E. Bothe, P. Chaudhuri. *Eur. J. Inorg. Chem.*, **10**, 1956 (2003).
[48] M. Sakamoto, S. Itose, T. Ishimori, N. Matsumoto, H. Okawa, S. Kida. *Bull. Chem. Soc. Jpn*, **63**, 6, 1830 (1990).
[49] A.P. Ginsberg. *J. Am. Chem. Soc.*, **102**, 111 (1980).
[50] L. Noodleman, C.Y. Peng, D.A. Case, J.-M. Mouesca. *Coord. Chem. Rev.*, **144**, 119 (1995).
[51] I. Ciofini, C.A. Daul. *Coord. Chem. Rev.*, **238**, 187 (2003).
[52] M. Buhl, H. Kabrede. *J. Chem. Theory Comput.*, **2**, 1282 (2006).